Pre, co and post-seismic motion for Altay region by GPS and gravity observations

V.Yu. Timofeev, D.G. Ardyukov, Y.F. Stus, E.N. Kalish*, E.V.Boiko, R.G. Sedusov, A.V. Timofeev, **B. Ducarme*

Trofimuk Institute of Petroleum Geology and Geophysics SB RAS, Novosibirsk, Russia.
**Institute of Automation and Electrometry SB RAS, Novosibirsk, Russia.*
***Royal Observatory of Belgium, Brussels, Belgium*

Abstract

We used GPS method to investigate the preseismic, coseismic and postseismic deformation due to the 27 September 2003, M_w = 7.3 Chuya (Altay) earthquake, which occurred south of Russian Altay mountains in southern Siberia near the Russia-Mongolia-China border. On the basis of GPS data measured during the campaigns of observation covering the period 2000-2007, we determined the magnitude and space distribution of 3D displacement fields for different epochs. Geodynamical GPS network consists of 23 sites and extends over structural elements of Russian Altay and surroundings territory (from 49.5°N to 54.8°N, from 81.2°E to 91.4°E). GPS data have been analyzed by GAMIT-GLOBK. Evidence was available of the existence of preseismic (2000-2003 years), coseismic (2003-2004 years) and postseismic (2004-2007 years) processes in this region. We used absolute gravity observation to check vertical motion at base points. Map of preseismic contemporary rates showed values from 0.5 to 10 mm/y and features in 3D velocity field. Russian Altay preseismic motion is connected with present-day displacement in West China and Mongolia. By analysis of the GPS data for 2003-2004 we got the map of coseismic displacements, reflecting the right-lateral strike-slip process in epicentral zone (130°N÷140°N orientation for rupture line). Coseismic horizontal displacements depend on distance between rupture line and GPS benchmarks position, for example, we obtained values from 350 mm at 15 km to 25 mm at 90 km. Vertical motion was smaller (10 ÷ 40 mm). GPS data for 6 benchmarks in epicenter zone show correlation with 2-D model with parameters - for jump on rupture line – 2 m, for maximal depth – 15 km, for shear strain 4 MPa. 3D modeling of coseismic process allowed us to understand displacement field for vertical motion at the end of earthquake rupture (10 ÷ 40 mm jump). Coseismic deformation on 10^{-6} level extended over the epicentral zone (100 km). Postseismic displacement field (2004-2007 years) showed the right-lateral motion in epicenter zone (3 ÷ 7 mm/y). Postseismic data allowed to develop a postseismic model for Chuya earthquake and to determine lower crust parameters (viscosity 10^{21} Pa·s). Analyses of 2000-2007 data allowed us to separate ongoing seismic motion from tectonic motion for West part of Russian Altay (2 mm/y to NW).

Key words: Pre, co- and post-seimic motion by GPS and absolute gravity, earthquake source parameters, viscosity-elastic model.

1. INTRODUCTION

Until recently crustal dynamics in the Altay-Sayan region could be investigated only by the classical geodetic techniques (transit or repeated leveling surveys) within local sites. Satellite surveys have been used since 2000 as part of international project “Present-day Deformation in the Altay-Sayan Region, Siberia, from GPS Geodesy, Absolute Gravimetry and Structural Analysis: Implications for Intracontinental Deformation Process in Central Asia” (grant 97-30874 from INTAS). The objectives of the project include the estimation of recent crustal movements and motions on faults, velocity and strain measurements, integration with data

acquired in the Tien Shan and Baikal region. It was expected to create a united GPS network from Tien Shan to the Baikal rift through East Kazakhstan and Altay-Sayan regions and to join Chinese GPS networks. Such network will record horizontal velocities over the greatest part of Asia and shed more light on the effect of India-Eurasia collision on current deformation in the southern surroundings of Siberia.

The Russian Altay and Sayan regions constitute the northern boundary of the active deformation zone of Central Asia, together with the Baikal rift zone further east. This major intracontinental tectonic feature is associated with strong seismic activity and surface deformations. The territory of Russian Altay is highly elevated area (up to 4500 m) with strike-slip faults, oblique thrusts, thrusts and normal faults. Analysis of earthquake focal mechanisms and stress tension inversion suggests in Altay-Sayan area two zones with different orientation of main stress axes [Peltzer&Saucier, 1996; Calais et.al., 2000, 2002, 2003]. To the east, in the Sayans, southern Tuva and northern Mongolia, a NNE-directed near horizontal compression dominates. To the west, in Russian Altay, a NNW-directed horizontal compression dominates. Last strong Chuya earthquake (27/09/2003, 49,999°N, 87,852°E, Mw = 7.3 ÷ 7.5) happened on Russian Altay territory where GPS network observations had been performed previously. Chuya (Altay) earthquake was the largest event striking the Russian Altay mountains in the last centuries. The objective of our study is to estimate pre-seismic, co-seismic and post-seismic velocity fields in the Chuya earthquake zone and in surroundings territory using GPS method. Choice of co- and post-seismic process models is the second task of our investigation. Third task is the estimation of tectonic part in Russian Altay velocity field (2000-2007 yy.).

2. ONGOING CRUSTAL MOVEMENTS IN RUSSIAN ALTAY (2000-2007 yy.)

We started GPS measurement in Russian Altay region, an area extending from 49°N till 55°N and from 80°E till 90°E, in 2000 (Fig, 1). Geodynamical GPS network consists of 25 sites where we use 3 GPS receivers Trimble 4700 simultaneously and 1 receiver Trimble 4700 at the permanent station NVSK not far from Novosibirsk. Most of the benchmarks are situated on bed rock. It should be noted that the deposits included permanent frosted ground in Chuya and Kurai depressions. Observations were always performed during the month of July to eliminate the seasonal influence [Timofeev et al., 2003, 2006]. This network results together with observations in surrounding territories were presented in our 97-30874/INTAS report [Calais at al, 2002, 2003]. We measured NNE displacements in Western China. East-direction motion for Center Mongolia and NW displacements for Eastern Kazakhastan. GPS measurements during four campaigns on the Altay network (2000-2003 yy.) were processed using Eurasian reference frame data (relative to 30 permanent stations) by the GAMIT-GLOBK software [Boucher et al., 2001]. The solution showed motion with respect to stable stations (NVSK, ELTS, KRUT) situated in a non deformed flat territory located at the north of Gorny Altay (Fig. 2). For this period the error was near 0.6 ÷1.0 mm for horizontal velocity and near 2.5 mm for vertical velocity. Most of the measured horizontal velocities were ranging from 0.2 to 4.0 mm/y and reach 5 ÷ 10 mm/y only for points in the extreme south. Note that the last measurement cycle ended in August 2003 just before the Chuya earthquake (M = 7.3, 27/09/2003) which struck the southern part of the studied territory [Goldin et al, 2003]. The fault plane solution for the Chuya earthquake indicated NS compression and EW extension. Vertical velocities before earthquake reflect this effect. We investigated the behavior of the north component of horizontal velocity along the S-N profile from the Lhasa station (LHAS, Tibet) to Novosibirsk (NVSK), through Urumchi (URUM, Western China), and epicenter area , i.e. along the direction orthogonal to the zone of active deformation in Asia. The velocities include northward component which changes linearly from 20÷22 mm/y at 29.6°N to 0÷2 mm/y at 55°N (Fig. 3). Velocities abruptly decrease after the UKOK benchmark (Ukok plateau, heights from 2500 m to 4000 m), i.e. in front of the future epicentral area. The preseismic NS velocities had been analyzed and have provided the deficit of

~ 5 mm/y at epicentral zone [this deficit noted too in Nissen et al, 2007]. The previous large earthquake in the Altay-Sayan region occurred about 250 years ago in this area. It was a M = 7.7 earthquake on 09/12/1761 at 50.0°N; 90.0°E [New catalogue, 1977] . Thus in the frame of linear model, the accumulated deficit of northward displacement is about 1,25 m or about 2 m in the nodal plane (2003, Chuya earthquake), which approximately corresponds to the seismic moment of 10^{20} N·m [http://neic.usgs.gov/neis/FM/neic-zfak-g.html]

The preseismic velocity field was studied and the existence of two dominant directions of motion (NW block and NE block) was shown in the studied territory (Fig. 2). The turn point for the NW and NE components was situated near Chuya earthquake epicenter. In the south the NE direction of motion agrees with GPS data for northwestern Mongolia (5-6 mm/y) and China (URUM, Urumchi, 11 mm/y). For deformation we can mention the NW extension of $5 \cdot 10^{-8}$ along the line of CHAG-KURA-ULAG-CHIK-SEMI-USTK and the NE compression up to $2 \cdot 10^{-7}$ along the line UKOK-CHAG-YAZU.

GPS measurements after the Chuya event started in the spring of 2004, just after melting ice-snow cover. In May we carried out measurements at two sites (KURA, CHAG) located in the epicentral area (Fig. 4) and one site (ARTB) at 300 km to north of the main shock. In July 2004 we observed Altay network (Fig. 5). Processed data from sites within 100 km of the main shock showed the greatest coseismic deformation in the epicentral area. Continued seismic process had produced the noise. The difference between the May and July results represents the afterslip delay (Fig. 4):5 mm in a 2.5 month period. The co-seismic jump indicated a right-lateral slip along the earthquake rupture. Our benchmarks are located from 15 km to 90 km mainly on NW flank of Chuya earthquake. The horizontal displacement depends on the distance from the nodal plane: it decreased from 0.35 m at 15 km to 0.02 m at 90 km away from the rupture. The rupture line orientation was obtained by KURA result (155° N) and by CHAG result (125° N) and the average value determined through KURA-CHAG GPS result is 140° N ± 15° is similar to seismological data [Nissen et al, 2008, http://neic.usgs.gov/neis/FM/neic-zfak-g.html, Starovoit et al., 2003]. Vertical jump reached its maximum (0.03÷0.05 m) near the fault (15÷35 km distance from earthquake rupture). These results correspond to the sum of seismic effects accumulated during one-year period (from July 2003 to July 2004). Horizontal component predominate over vertical displacements for co-seismic motion. Analysis of the May-July-2004 data have shown that most of elastic effect took place during the first months after Chuya earthquake. The first-order effects, which correspond to a right-lateral strike slip, can be interpreted in the frame of the elastic rebound model. The applicability of the elastic rebound model is supported by the evidence of NW motion before the event (Fig 2, 5).

Postseismic velocity field was obtained for epicentral area during the 2004-2007-period (Fig. 5, Table 1). Postseismic motion presented the same sign as coseismic effect with smaller rate. Average velocity for epicenter area is 4÷5 mm/y (CHIB, AKTA, ULAG, KURA, CHAG) at distances ranging from 15 km to 50 km, average distance 35÷40 km.

Absolute gravity observation at NVSK, USTK and KAYT station were used to check vertical displacements for Altay network. Absolute gravity data were processed with corrections (tidal, polar motion, air pressure and other) recommended by International Center [Stus et al., 1995]. Results for Altay station USTK located on bed rock is presented on Fig. 6. Gravity value was stable in the range of standard error (2 microgal). This stable station was used as base point.

Some reports [Nissen et al., 2007, Barbot et al., 2008] presented SAR result for Chuya earthquake quoting 1 m vertical displacement near fault rupture line. This effect may be connected with landslip activity at Chuya-Kurai ranges side of rupture zone [Starovoit et al., 2003] and partly with lifting of permanent frozen ground at Chuya-Kurai depressions side. Weather anomaly was observed during the summer before Chuya earthquake and during the next winter. Usually Chuya-Kurai depressions and surrounding territory has very dry summer and winter condition like desert, but 2003-summer and 2003/2004 winter had rainy weather condition.

Processing of Russian Altay network data for 2000-2007 yy. period without the epicenter area results are shown on Fig. 2. This analyses allowed us separate seismic motion and tectonic part for West part of Russian Altay (2 mm/y to NW). This motion may be only a part of Russian Altay compression (5 ÷ 7 mm/y), other part may be included in the NE and East motion of Sayan-Tuva region situated at the East of Russian Altay.

3. MODEL OF COSEISMIC PROCESS AND CHUYA EARTHQUAKE SOURCE PARAMETERS

Current GPS velocities show for Russian Altay a shortening at 5÷7 mm/y level. Lying around 2500 km north from the Himalaya, the Russian Altay mountains comprise the most distant region of active continental shortening at 35÷45 mm/y level in the India-Eurasia collision zone. Most authors regard the Asian earthquakes process as the result of this effect. At a tectonic scale shortening would be realized partly by means of earthquake effect.

For strike-slip earthquake process the elastic rebound model appeared already one century ago [Reid, 1911; Stacey, 1969]. In a strictly elastic earth, complete elastic rebound would take place in a few seconds the only slow deformation would be the accumulation of tectonic strain. But single series GPS or SAR observations separated of some months period, and seismic process would study as a sum of main shocks, aftershocks and afterslip effect (Fig. 4). Our GPS network have not such a data density as SAR method, its benchmarks are situated far from earthquake rupture, but cover a more extensive territory.

We discussed this process for Chuya earthquake in frame of elastic theory at half space [Nur&Mavko, 1974; Savage&Burford, 1993; Segall, 2002; Turcott&Schubert, 1982]. Coseismic deformation can be explained by simple models based on solutions in an elastic half-space. When we have strike-slip events along subvertical rupture, with a length (***L***) much larger than the depth (***a***) or ***L*** >> ***a***, we can use 2D model (infinite length).

For Screw Dislocation Model (SDM, single source, Figure 7) the horizontal displacement $\Delta\omega_z$ along axis X on the surface can be written as

$$\Delta\omega_z = (\Delta\omega/2) \cdot [1 - (2/\pi) \operatorname{arctg} (x/a)]. \quad (1)$$

where $\Delta\omega$ is the slip in the fault plane.

In the next 2-D Model (2DM, source is infinite belt, Figure 8) we have strike-slip motion along the vertical infinite fault (along axis Z) at depth ***a*** (axis Y). For half-space (y>0) we have equilibrium equation for force along axis Z:

$$\partial\sigma_{xz}/\partial x + \partial\sigma_{yz}/\partial y = 0,$$

or for motion ω_z we have Laplace equation:

$$\partial^2\omega_z/\partial^2 x + \partial^2\omega_z/\partial^2 y = 0. \quad (2)$$

At the surface we have a distribution of the displacement along axis X depending from two parameters – depth (***a***) and slip along the crack ($\Delta\omega = (\sigma_{xz,0}/G)\cdot 2\boldsymbol{a}$) :

$$\Delta\omega_z = \pm\Delta\omega \cdot [(1 + x^2/a^2)^{1/2} - |x|/a] / 2. \quad (3)$$

The effects for these models (SDM and 2DM) are quite similar (Fig. 9). Two parameters (the slip - $\boldsymbol{\Delta\omega}$ and the depth – ***a***) control displacement distribution. If we take GPS results for coseismic jumps at different distances from main shock (27/09/2003), earthquake source parameters ($\boldsymbol{\Delta\omega}$ and ***a***) can be computed by SDM and 2DM. Using results for CHAG and YAZU points we received $\boldsymbol{\Delta\omega}$ = 1.7 m, ***a*** = 8.6 km (SDM) and $\boldsymbol{\Delta\omega}$ = 1.9 m, ***a*** = 10.0 km (2DM). Second solution is more correct for our annual GPS observation as it include aseismic creep and afterslip effect. These results are in good agreement with seismological results. Similar displacement curve for Chuya earthquake coseismic displacements across fault was obtained by InSAR method [E.Nissen at al., 2007]. It is known that the seismological estimations of Chuya earthquake coordinates differ up to 10÷20 km due to unknown crust parameters for this region.

At next steps of analyses we used 130°N orientation of subvertical nodal plane, which crossed the main shock point with coordinates (49,999°N, 87,852°E), for parallel displacement

calculation. The results for 2D model and experimental results are shown at Figure 10. Using experimental GPS data for center of zone (CHAG and KURA) and theoretical distribution (2DM, (2)) we can determine parameters $\boldsymbol{a}$ and $\boldsymbol{\Delta\omega}$. In this case we have: $\boldsymbol{a}$ = 16.5 km and $\boldsymbol{\Delta\omega}$ = 1.8 m. The same value for slip was received by seismological study (2 m) and by geomorphology data (0.5 ÷ 5.0 m).

For elastic modulus G values ranging from 30 GPa to 55 GPa, depth from 9 km to 16 km and displacement 2 m we have estimated the shear stress range - from 2 MPa to 6 MPa, and the average - 4 MPa.

This method (2DM) was tested successfully for Western Kunlunshan Pass region where strong earthquake (M = 8.1) with left-lateral slip (5 ÷ 7 m) happened on 14.11.2001 [X. Shan, 2004]. In this case mean value for depth agree with seismological data too.

For Chuya earthquake using slip value ($\Delta\omega$ = 2 m) we tested the depth value in different part of epicenter zone (figure 10) and estimated the length of the fault (140 km). Depth reduced from 15 km (at the center) up to 0 km at the ends of nodal plane. Using this model the frames of shift deformation were calculated (Figure 9). Co-seismic deformation for triangles: UKOK-CHIK-KAIT; CHAG-KURA-YAZU; KURA-BALY-YAZU; ULAG-KURA-BALY, was estimated by GPS results (Figure 11). Coseismic deformation on 10^{-6} level extends over epicentral area (near 100 km from the main shock epicenter).

For study of 3D coseismic jump and for vertical displacement especially at the ends of the rupture we used 3-D model [Okada, 1985]: vertical finite shear fault with constant slip (2 m), spatial depth's distribution and 140 km length of fault at the surface. This solution is surface integration of single source (see formula (1)) Calculation are carried out with normal Poisson's ratio (ν = 0.25). Fault model consists of three planes, the origin (0, 0) being at the epicenter of main shock (27/09/2003):

1. for 0 < a < 5 km, L = 130 km, from -57 km to +73 km;
2. for 5 < a < 10 km, L = 97 km, from -46 km to +51 km;
3. for 10 < a < 15 km, L = 42 km, from -20 km to +22 km.

The results correspond to our experimental data, for example, station UKOK:
model (x, y, **z**) 246.9 mm, 96.2 mm and **25.6 mm** (265 mm vector)
and the experiment (x, y, **z**) 204.0 mm, 192.5 mm and **28.7 mm** (280 mm vector)).
Differences are connected with the nodal plane location at the end of the rupture and the non vertical position of nodal plane at the end of earthquake rupture.

Using the above mentioned 3-planes model (slip 2m and G = $3.3 \cdot 10^{10}$ Pa), earthquake source parameters were determined: seismic moment $M_0 = 0.9 \cdot 10^{20}$ N·m, earthquake magnitude $M_w = 7.2$ ($M_w = \frac{1}{2}(\log M_0 - 5.5)$).

We can compare earthquake magnitude and rupture length by empirical scaling relationships between magnitude and surface rupture length. Authors [Johnson&Segall, 2004] suggest magnitude, M_w, and rupture length, L, are related as

$$M_w = 1.1 \cdot \log (L) + 5.0 \qquad (4)$$

Using this relationship, Chuya earthquake with a rupture length in the range 75 ÷ 140 km would have a magnitude in a range M_w = 7.0 ÷ 7.4.

4. POSTSEISMIC DISPLACEMENT (2004 - 2007 yy.) AND VISCOELASTIC MODELS

We used GPS network to study the postseismic transients. The postseismic displacement field (2004-2007, Table 1) has the same sign as the coseismic one (Figure 5). The observed postseismic signal extends from epicenter zone, with wavelengths much larger than locking depth (8 ÷ 16 km), but of the order of the fault length (80 ÷ 150 km). As noted by [Barbot et al, 2008] the polarity of the postseismic displacement around the fault does not warrant the poroelastic rebound in the upper crust, suggesting a very low permeability or fluid saturation of the crustal rocks in the Chuya&Kurai depressions and Chuya Range. Concerning the possibility

of a rapid pore fluid flow within the first seven months following the earthquake, we have no constraints from our GPS data. We cannot rule out the afterslip process during the first year following the earthquake as it was discussed [Barbot et al, 2008]. This effect can be present at May-July 2004 result (Figure 4).

The screw dislocation or 2DM provides only a very limited description of plate-boundary faulting. A somewhat more realistic model involves an elastic layer of thickness H overlying a Maxwell viscoelastic half-space [Segall, 2002]. The Maxwell material has relaxation time $\tau_R = 2\eta/\mu$, where η is the viscosity and μ is the shear modulus. At time t = 0 slip Δu occurs on the fault from the surface to depth $D \leq H$. The velocity on the Earth's surface as a function of position perpendicular to the faults, x, number of seismic activity process, n, and time, t, is

$$v(x, t) = (\Delta u/\pi\cdot\tau_R)\cdot \exp(-t/\tau_R) \sum_{n=1}^{\infty}[(t/\tau_R)^{n-1}/(n-1)!]\cdot F_n(x, D, H), \qquad (5)$$

where the spatial distribution is given by

$$F_n(x, D, H) = [\tan^{-1}(D+2nH/x) + \tan^{-1}(D-2nH/x)] = \tan^{-1}[2xD/x^2+ (2nH)^2- D^2],$$

if n =1

$$v(x, t) = (\Delta u/\pi\cdot\tau_R)\cdot \exp(-t/\tau_R) \tan^{-1}[2xD/x^2+ (2nH)^2- D^2]. \qquad (6)$$

The post-seismic velocity is a function of the coseismic slip Δu, the depth of faulting D, the elastic layer thickness H, the material relaxation τ_R and the time since the last large earthquake t.

The temporal dependence depends only on the dimensionless ration t/τ_R and relaxation time τ_R (see Fig. 12, $(\Delta u/\pi\cdot\tau_R)\cdot \exp(-t/\tau_R)$). The spatial distribution is given by a function of position perpendicular to the faults, x, the depth of faulting D, and the elastic layer thickness H (see Fig. 13, $\tan^{-1}[2xD/x^2+ (2nH)^2- D^2]$). From parameters presented at Table 1 (3-4 mm/y for epicenter zone), at Fig. 12 and 13 we can estimate Maxwell time $\tau_R \geq 100$ years.

A model of viscoelastic relaxation is convenient to describe postseismic effect of Chuya earthquake. In order to determine the characteristics of time-dependent deformation which follows the sudden slip on large earthquake faults, one considers two-layers in the crust, an elastic layer H overlying a viscoelastic layer h (Elsasser model, Figure 14). Assuming that at time t = 0 sufficient tectonic stress has accumulated to cause sudden faulting, the solution to the elastic-viscoelastic model was obtained in two steps: first the static displacements were solved and stresses due to a fault in an elastic layer welded to an viscoelastic layer. But, as time goes on, the deformation changes as a result of the relaxation in lower viscoelastic layer, formal effect is like an earthquake source drop. Important parameters for viscoelastic model are stress jump, earthquake depth, thickness of elastic layer and viscoelastic layer, elastic modulus and viscoelastic modulus, rate of deformation or motion, elapsed time since the event, velocity at surface at different distances from the epicenter and nodal line. Usually two-layers model is used. As shown in the papers [Barbot, 2008; Wang et al., 2003] three-layers model with weak mantle does not change results insignificantly. Two layers model used following parameters: elastic layer (thickness H), viscous layer (thickness h) and the fault along axis Z; right-lateral postseismic velocity ($\partial\omega_{zE}/\partial t$), stress jump σ_{xz}. We consider in the two-layers model a 20 km elastic upper crust and a 25 km viscoelastic lower crust [Elsasser, 1971, Calais et,al, 2002]. Preliminary result for post-seismic average velocity observed at distance range 15÷50 km was estimated as 5 mm/y, the stress jump for Chuya earthquake was estimated as 4 MPa, elastic modulus for crust G = 33÷55 GPa. For the viscosity of lower crust we have:

$$\eta = \sigma_{xz}\cdot h / (\partial\omega_{zE}/\partial t) = 5\div 8\cdot 10^{20}\ \text{Pa}\cdot\text{s}, \qquad (7)$$

Relaxation time for Russian Altay (Elsasser time $\tau = \eta/2G$) was estimated as 200÷300 years. Elsasser time and Maxwell time connect by equation [Elsasser, 1969]:

$$\tau_M = [\pi^2 \cdot H/(16h)] \cdot \tau_E, \quad (8)$$

for our parameters (H =20 km and h = 25 km) we have $\tau_M = 0.49 \cdot \tau_E$.

These parameters corresponded to two-layers model with the largest wavelength of the deformation [Barbot et al, 2008].

5. CONCLUSIONS

GPS observations show NW motion in Western part of Russian Altay (2 mm/y), as a part of NNE convergence (7 mm/y) is accommodated across the Russian Altay mountains. Present-day velocity field is deformed in its south-east part by Chuya earthquake process. Features in velocity field before Chuya earthquake were obtained by GPS networks. Future epicenter was located at the junction between NW group and NE group of motion. Anomalous horizontal velocities were measured in southern part of Russian Altay at 3÷10 mm/y level. Vertical velocities have shown an increase to the north of the epicenter and a decrease to the south of the epicenter. In the frame of linear tectonics we had accumulation of horizontal displacement before Chuya earthquake (2 meters). Coseismic displacements reflected the right-lateral jump in epicenter zone with determined rupture orientation 140° N ± 15°. Coseismic displacement depended from the distance between nodal plane and GPS benchmarks (from 350 mm (at 15 km) to 25 mm (at 90 km)). 2-D model for surface displacements have been used to describe these phenomena. Using experimental data and modeling, we have estimated parameters of earthquake source: for slip – 2 m, for maximal depth – 15 km, for rupture length – 140 km, for shear stress - 4 MPa, for seismic moment - $0.9 \cdot 10^{20}$ N·m and for magnitude M = 7.2. Preliminary results for post-seismic process show a right-lateral motion with velocity near 4 mm/y. Using two layers model (brittle-elastic upper crust and viscoelastic lower crust) the estimation for effective lower crust viscosity is: $8 \cdot 10^{20}$ Pa·s. Relaxation time in this case was estimated as 300 years.

References

Barbot S., Hamiel Y., Fialko Y., 2008, Space geodetic investigation of the coseismic and posrseismic deformation due to the 2003 M_w 7.2 Altay earthquake: Implications for the local lithospheric rheology. // Journal of Geophysical Research, v.113, B03403, doi: 10,1029/2007JB005063.

Boucher C., Altamimi Z., Sillard P., Feissel-Vernier M.. (2001) The ITRF 2000. // IERS Technical Note, 2001, No.31., 270 p..

Calais E., Amarjargal S., 2000, New constraints on current deformation in Asia from continuous GPS measurements at Ulan Baatar, Mongolia. // Geoph. Res. Letters, v. 27, No. 10, 1527-1530.

Calais E., Vergnolle M., Deverchere J., 2002, Are post-seismic effects of the M 8.4 Bolnay earthquake (1905 July 23) still influencing GPS velocities in the Mongolia-Baikal area? // Geophys. J. Int., 149, 157-168.

Calais E., Vergnolle M., San'kov V., Lukhnev A., Miroshnichenko A., Amarjargal S., Deverchere J., 2003, GPS measurements of crustal deformation in the Baikal-Mongolia area (1994-2002): Implications for current kinematics of Asia. // J. Geophys. Res., 108 (B10), 2501, doi: 10,1029/2002JB002373.

Elsasser W.H., Convection and stress propagation in the upper mantle. // "The Application of Modern Physics to the Earth and Planetary Interior, ed. Runcorn, S.K., Wiley, New York, 1969, 223-246.

Elsasser W.H., Two-Layer Model of Upper-Mantle Circulation. // J. Geophys. Res., 1971, v.74, n.20, p.4744-4753.

Fialko Y., 2004, Evidence of fluid-filled upper crust from observations of postseismic deformation due the 1992 M_w 7.3 Landers earthquake. // Jour.Geophys.Res., v.109, B08401, doi.:10.1029/2004JB002985.

Freed A.M., Burgmann R., Calais E., Freymueller J., Hreinsdottir S., 2006. Implications of deformation following the 2002 Denali, Alaska, earthquake for postseismic relaxation processes and lithopheric rheology. // Jour.Geophys.Res., v. 111, B01401, doi.:10.1029/2005JB003894.

Goldin S.V., Timofeev V.Y., Ardyukov D.G. Fields of the earth's surface displacement in the Chuya earthquake zone in Gornyi Altay. // Doklady Earth Sciences, vol.405A, No.9, 2005, 1408-1413.

Johnson K.M., Segall P., 2004,Viscoelastic earthquake cycle models with deep stress-driven creep along the San Andreas fault system. // Journal of Geophysical Research, v,109, B10403, doi: 10,1029/2004JB003096.

Nissen E., Emmerson B., Funning G. J., Mistrukov A., Parsons B., Robinson D.P., Rogozhin E., Wright T.J., 2007, Combining InSAR and seismology to study the 2003 Siberian Altay earthquakes – dextral strike-slip and anticlockwise rotations in the northern India-Earasia collision zone. // Geophys, J, Int, , 169, 216-232, doi: 10,1111/j, 1365-246X, 2006,03286,x.

Nur A., Mavko G., 1974, Postseismic Viscoelastic Rebound. // Science, v. 183, n. 4121, 204 – 206.

New catalogue of historic strong earthquakes for the USSR territory, from oldest time to 1975. (in Russian) 1977, Nauka, Moscow, 297-314.

Okada Y., 1985. Surface deformation due to shear and tensile faults in a half-space. // Bull. Seismol. Soc. Am., 75, 1135-1154.

Peltzer G., Saucier F. (1996) Present-day kinematics of Asia derived from geologic fault rates. // J.Geophys.Res., December 10, 1996, v.101, B12, pp.27,943-27,956.

Reid H. F. (1911) The elastic rebound theory of earthquakes. // Bull. Dept. Geology. Univ. California, 1911, 6, 413 p..

Savage J.C., Burford R.O., 1973, Geodetic Determination of Relative Plate Motion in Central California. // Journal of Geophysical Research, v. 78, No. 5, pp. 832-835.

Savage J.C., Prescott W. H., 1978, Asthenosphere Readjustment and the Earthquake Cycle. // Journal of Geophysical Research, v, 83, No, B7, 3369-3376.

Segall P., 2002, Integrating Geologic and geodetic Estimates of Slip Rate on the San Andreas Fault System. // International Geology Review, v, 44, p, 62-82.

Stacey F.D., Physics of the Earth, 1969, J.W.&S.I., New York, London, Sydney, Toronto, 342 p..

Starovoit O.E., L.S.Chepkunas, I.P.Gabsatarova, 2003,The parameters of earthquake 27/09/2003 at Altay by instrumental data. (In Russian). // Electronic Journal of Science and Information magazine, "Vestnik otdelenia nayk o Zemle RAN"(Bull. RAS, Earth Sci.), n.21.

Stus Y.F., Arnautov G.P., Kalish E.N., Timofeev V.Y., 1995, Non-tidal Gravity variation and Geodynamic Processes. // "Gravity and Geoid", Shpringer, Germany, p.35-43.

Timofeev V. Yu., Ardyukov D.G., Duchlov A.D., Zapreeve E.A., Calais E., 2003, Modern geodynamics of western Altay-Sayan region, from GPS data. // Russian Geology and Geophysics, 44, 1168-1175.

Timofeev, V, Yu,, Ardyukov D,G,, Calais E,, Duchlov A,D,, Zapreeve E,A,, Kazantsev S,A,, Roosbeek F,, Bruyninx, 2006, Displacement fields and models of current motion in Russian Altay. // Russian Geology and Geophysics, 47, n.8, 923-937.

Timofeev, V, Yu, Gornov P.Y., Ardyukov D,G, Malishev Yu.F., Boyko E.V. Results of analysis GPS data (2003-2006 yy.) at Sikhote-Alin net, Far East. // Geology of the Pacific Ocean, v.27, n.4, 2008, p. 39-49 (ISSN 0207-4028).

Turcott D.L., Schubert G., 1982, Geodynamics. Applications of Continuum Physics to Geological Problems. John Willy & Sons. 2 v., New York, Chichester, Brisbane, Toronto, Singapore, 730 p.

Wang R., Martin F.L., Roth F., 2003, Computation of deformation induced by earthquakes in a multi-layered elastic crust-FORTRAN programs EDGRN/EDCMP. / Computers&Geosciences, 29, 195-2007.

Xinjian Shan, Jiahang Liu, Chao Ma, 2004, Preliminary Analysis on Characteristics of Coseismic Deformation Associated with M=8.1 Western Kunlunshan Pass Earthquake in 2001. // Proceedings of the APSG Symposium. Space geodesy and its applications to Earth Sciences, Shanghai Astronomical Observatory, CAS, p.91-98.

Table 1. Velocities for Altay network (2004-2007 yy.) calculated relative Eurasia plate model AR-IR2006 [Timofeev et.al., 2008]. Epicenter zone – red. West part of Gornii Altay – green

Code of point	Latitude φ	Longitude λ	Height, m, WGS84	AR-IR 2006, Vφ	AR-IR 2006, Vλ	Exper. Vφ	Exper. Vλ	Difference Vφ	Difference Vλ
UKOK	49,562° N	88,232° E	2323.9	-3.64	26.26	-2.0±0.8	24.6±0.7	+1.6±0.8	-1.6±0.7
KURA	50,245° N	87,890° E	1490.3	-3.54	26.22	-6.8±0.5	30.0±0.6	-3.2±0.5	3.8±0.6
CHAG	50,068° N	88,417° E	1710.6	-3.69	26.21	-7.9±0.4	30.0±0.5	-4.2±0.4	3.8±0.5
AKTA	50,325° N	87,619° E	1365.5	-3.50	26.20	-7.8±1.3	30.1±1.1	-4.2±1.3	3.9±1.1
CHIB	50,313° N	87,503° E	1122.8	-3.43	26.23	-7.7±0.8	27.0±0.9	-4.2±0.8	0.8±0.9
								-3.9	**+3.1**
YAZU	50,586° N	88,851° E	1542.8	-3.82	26.14	-10.2±1.2	34.6±1.3	-6.3±1.2	8.4±1.3
ART2	51,799° N	87,282° E	460.8	-3.36	26.09	-3.6±0.5	26.8±0.5	-0.2±0.5	0.7±0.5
CHIK	50,644° N	86,313° E	1249.5	-3.08	26.25	-0.9±0.3	23.3±0.3	+2.1±0.3	-3.0±0.3
USTK	50,939° N	84,769° E	999.4	-2.63	26.28	-2.3±0.3	24.3±0.3	+0.3±0.3	-2.0±0.3
KAYT	50,146° N	85,439° E	1037.5	-2.83	26.33	0.7±0.3	23.4±0.4	+3.5±0.3	-2.9±0.4
								+1.9	**-2.6**

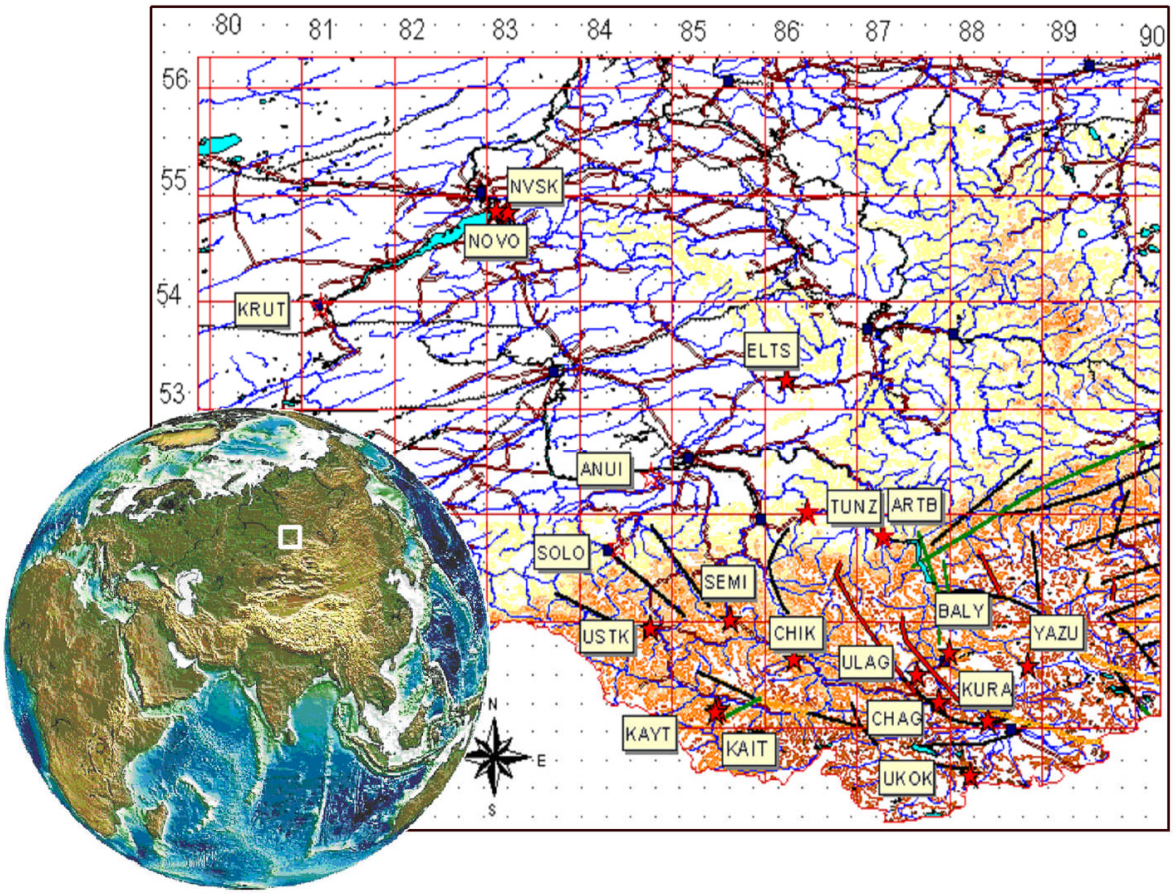

Figure 1: GPS stations in Gorny Altay and reference stations to the North

Pre-seismic situation and tectonic part

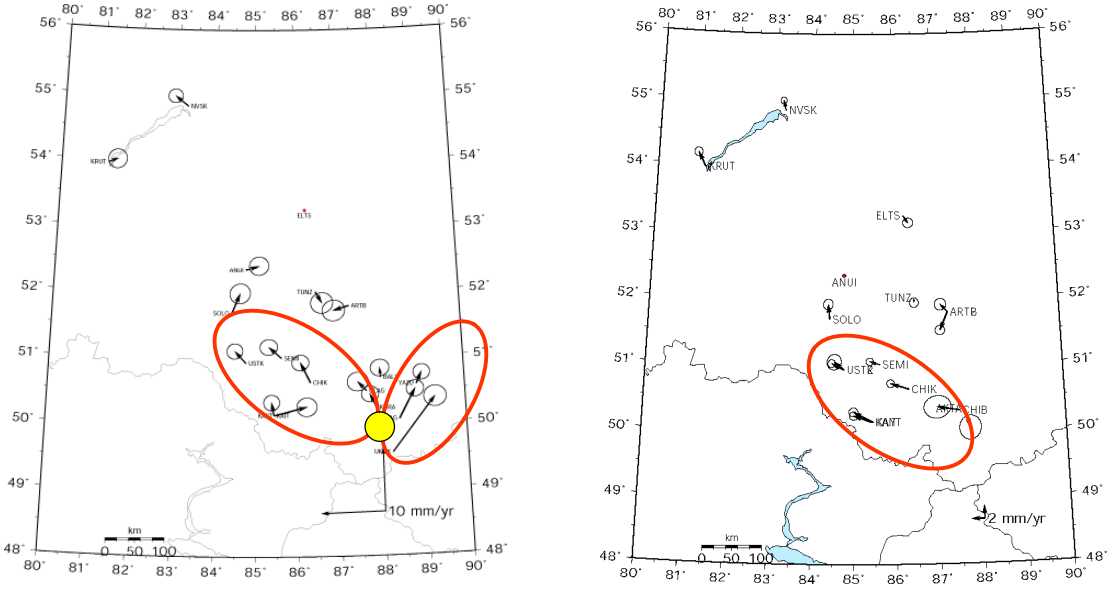

2000-2003 **2000-2007**

Figure 2: Pre-seismic situation (2000-2003) and long term tectonic part (2000-2007)

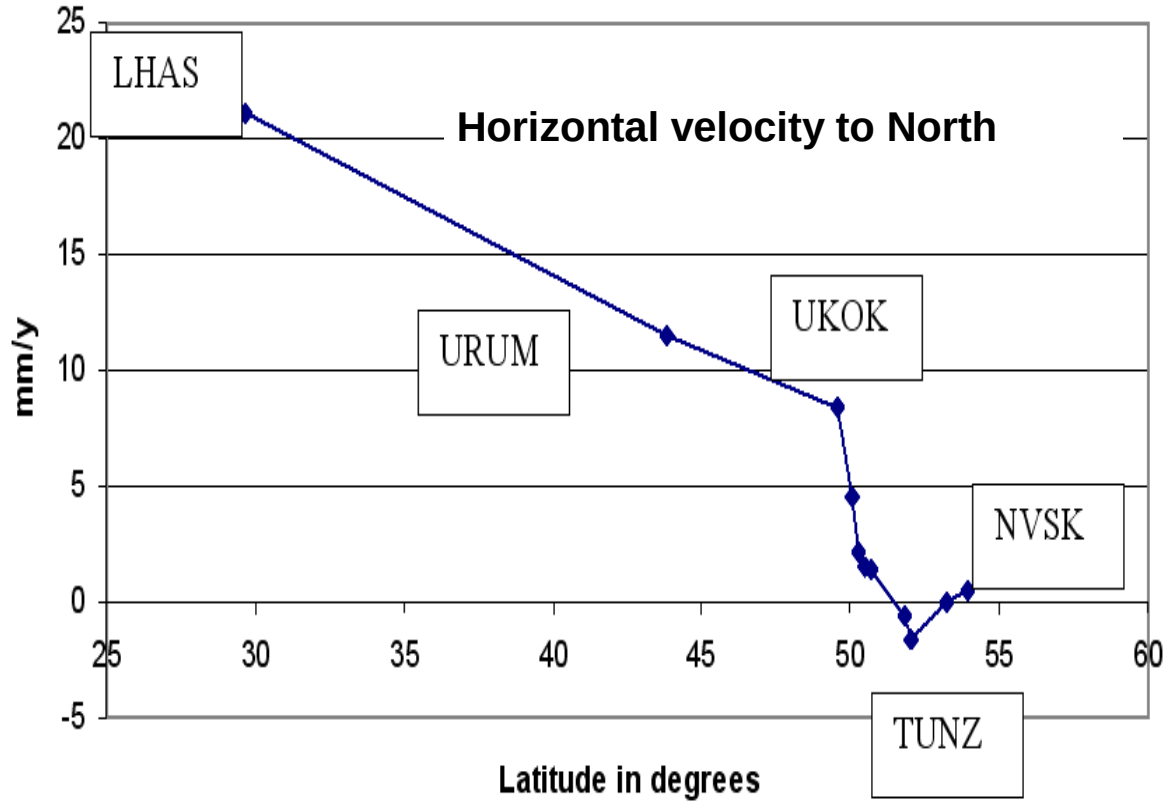

Figure 3: Horizontal velocities along a SN profile Lhasa-Novosibirsk

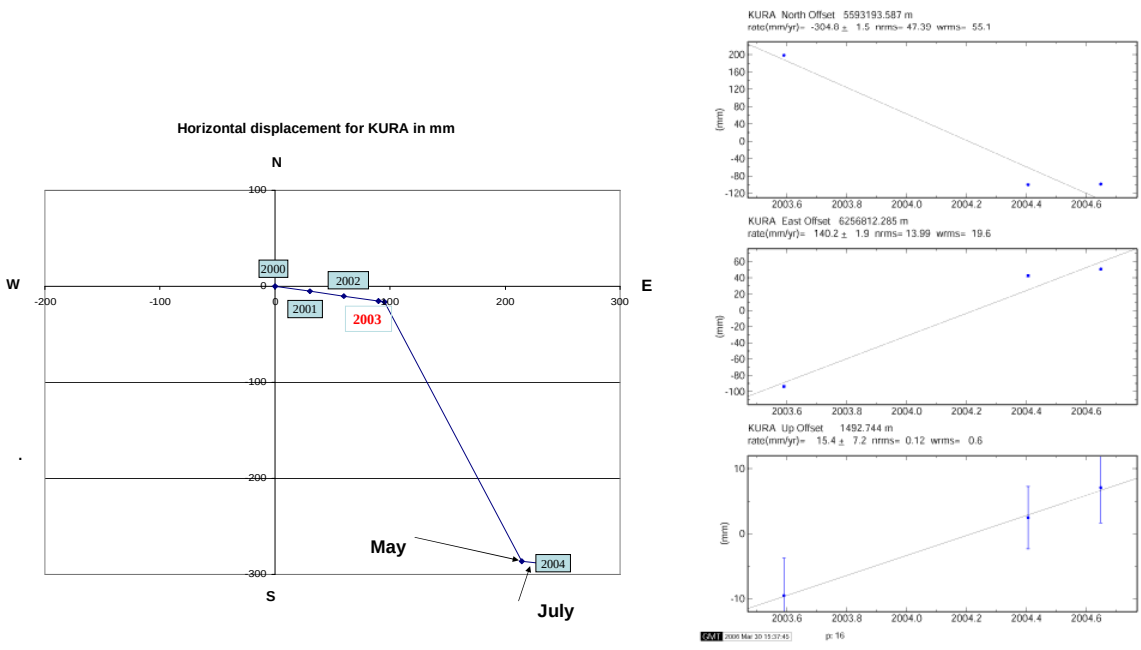

Figure 4: Coseismic jump measured at KURA station due to Chuya earthquake

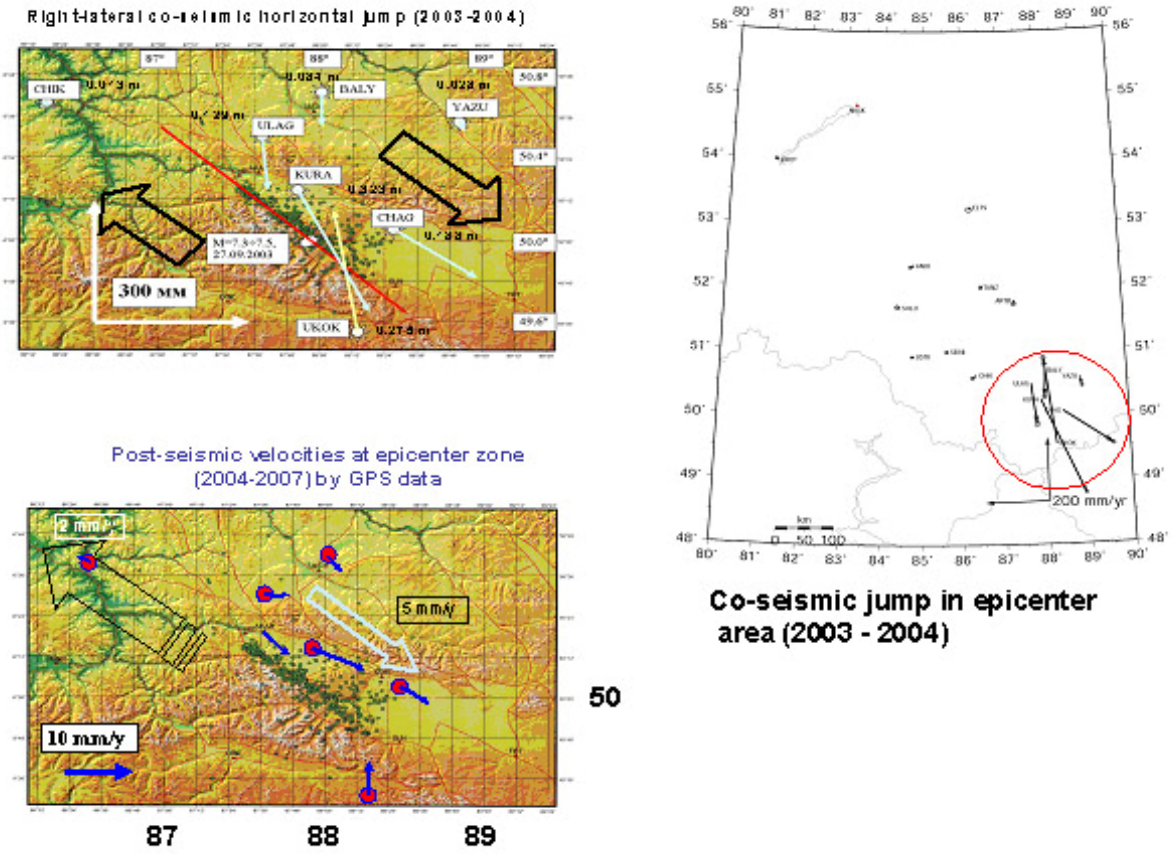

Figure 5: Co- and post-seismic deformation in epicentral area observed with Altay network

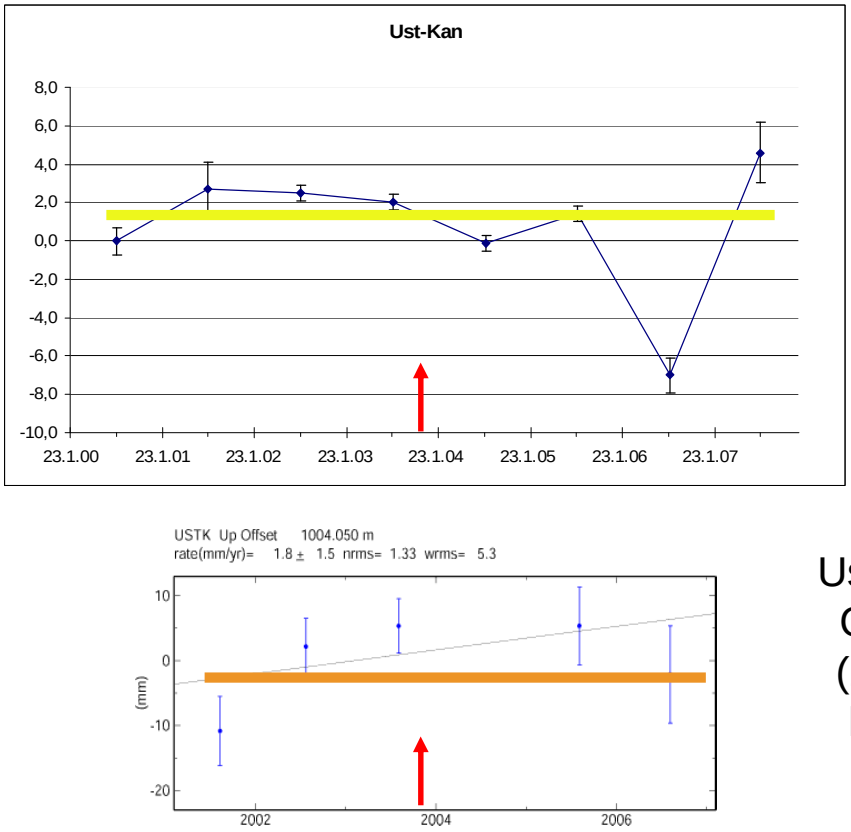

Ust-Kan, bed rock. Gravity variation (2000-2007) and height variation (2001-2006)

Figure 6: Comparison of gravity changes (μgal) and height variations (mm) at Ust-Kan station

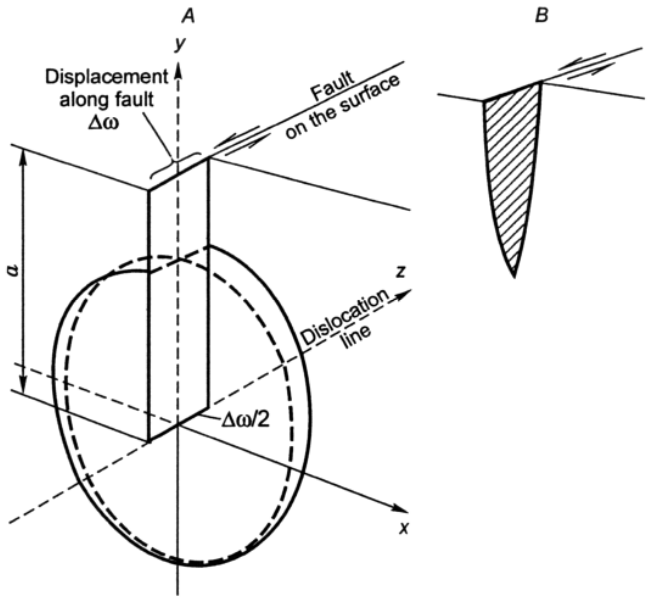

Figure 7. Screw Dislocation Model (SDM, single source).

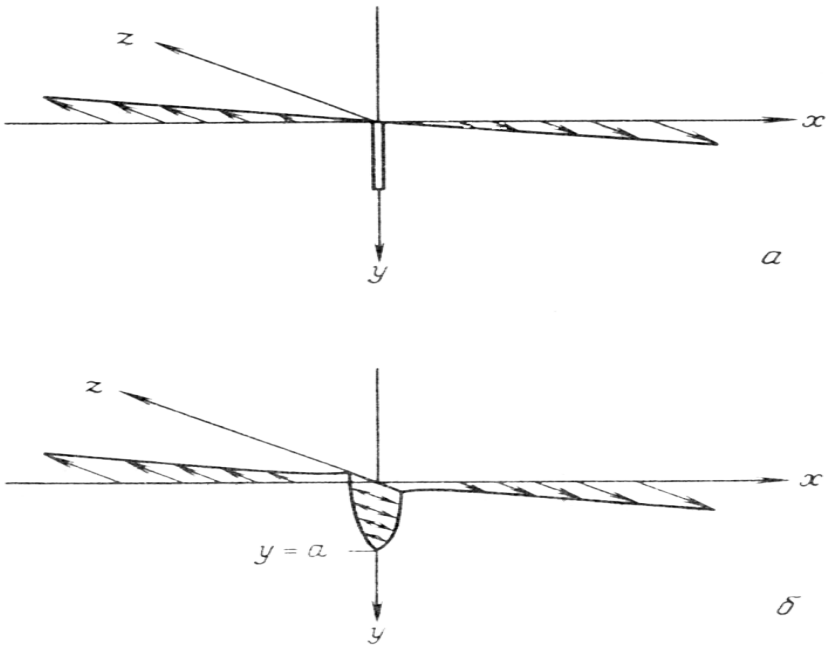

Figure 8. a) 2D Model; b) 2DM, belt source).

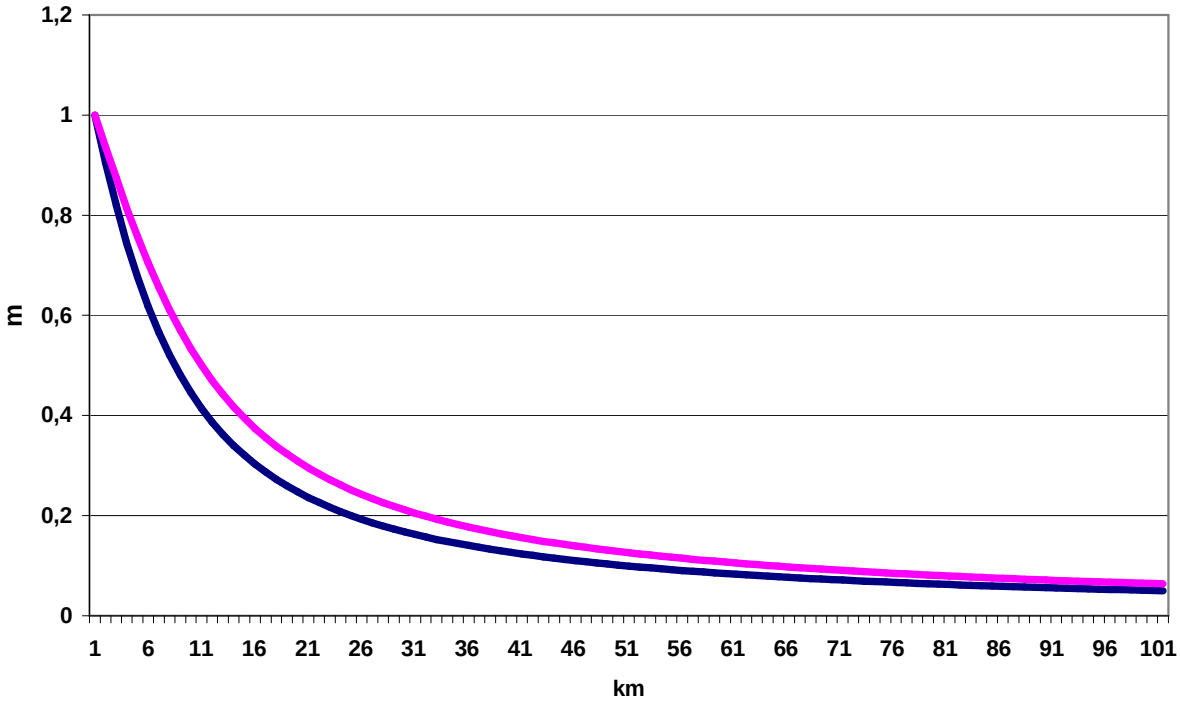

Figure 9: Dislocation according to distance to the rupture plane using SDM and 2DM models

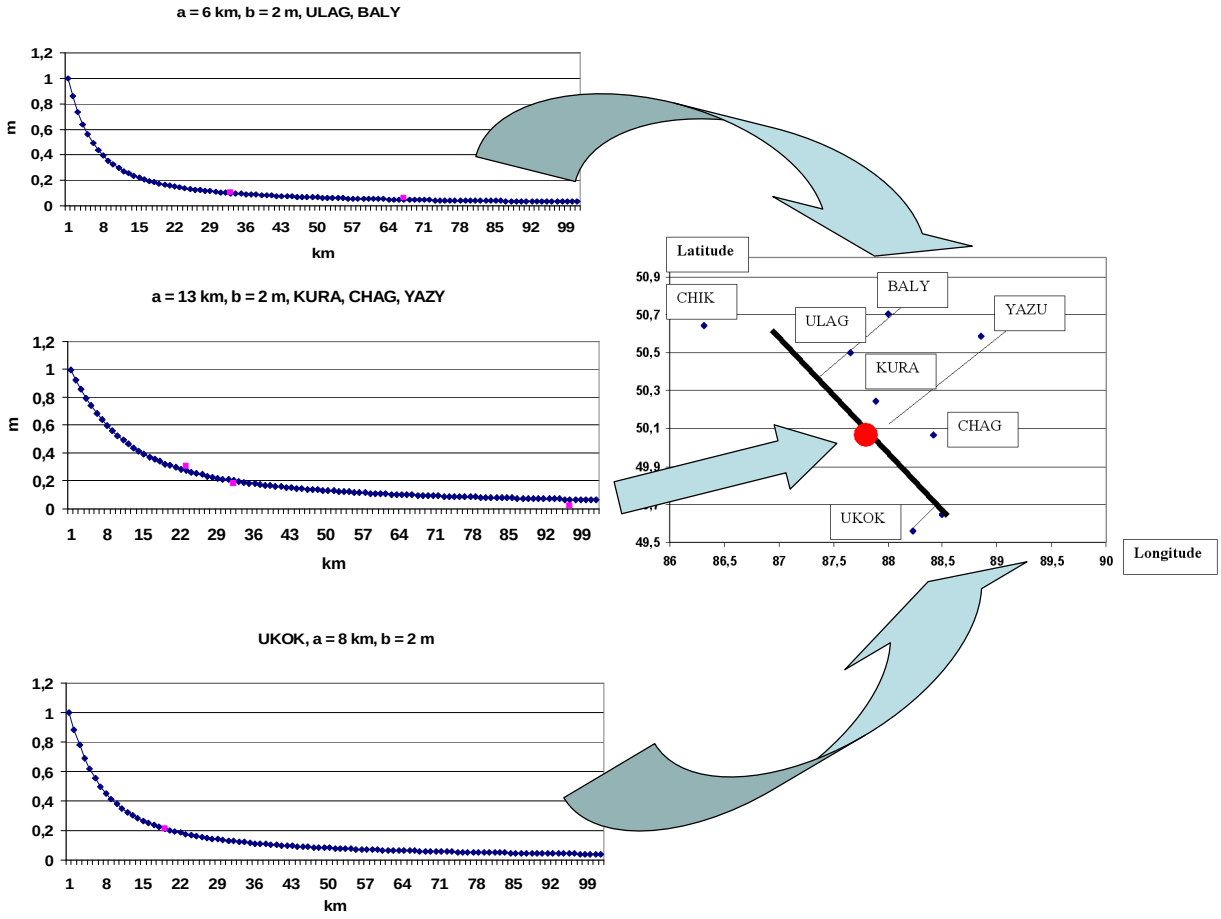

Figure 10: Displacement curves parameters a (depth) and b (slip) determined from the GPS observations (red dots) at different stations using the 2DM model.

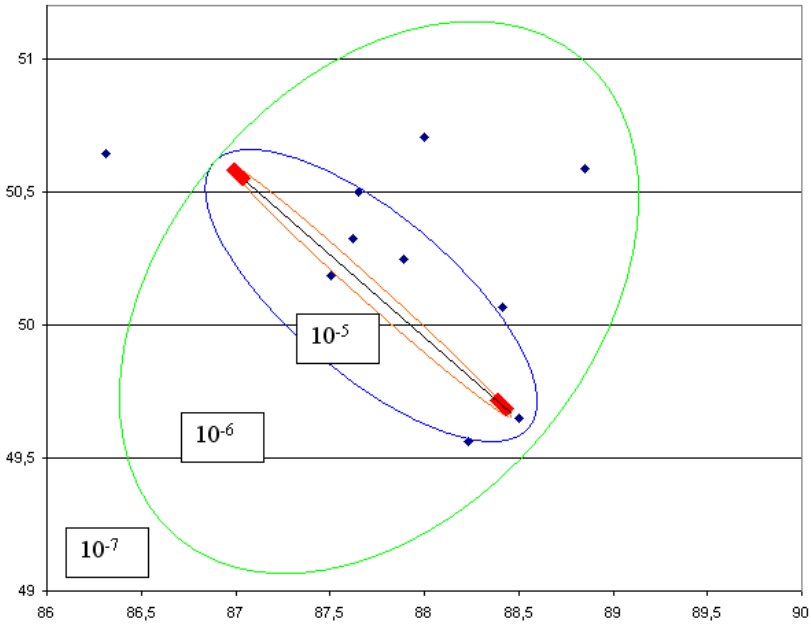

Figure 11: Coseismic shift deformation by 2D model with changing depth, symmetrical change by epicenter (from 15 km to 1 km, deformation Uxy, step - 1 km). Axes are labeled according to latitude and longitude. 10^{-7}, 10^{-6}, 10^{-5}, 10^{-4}, deformed zone up to10^{-3} at the end of line.

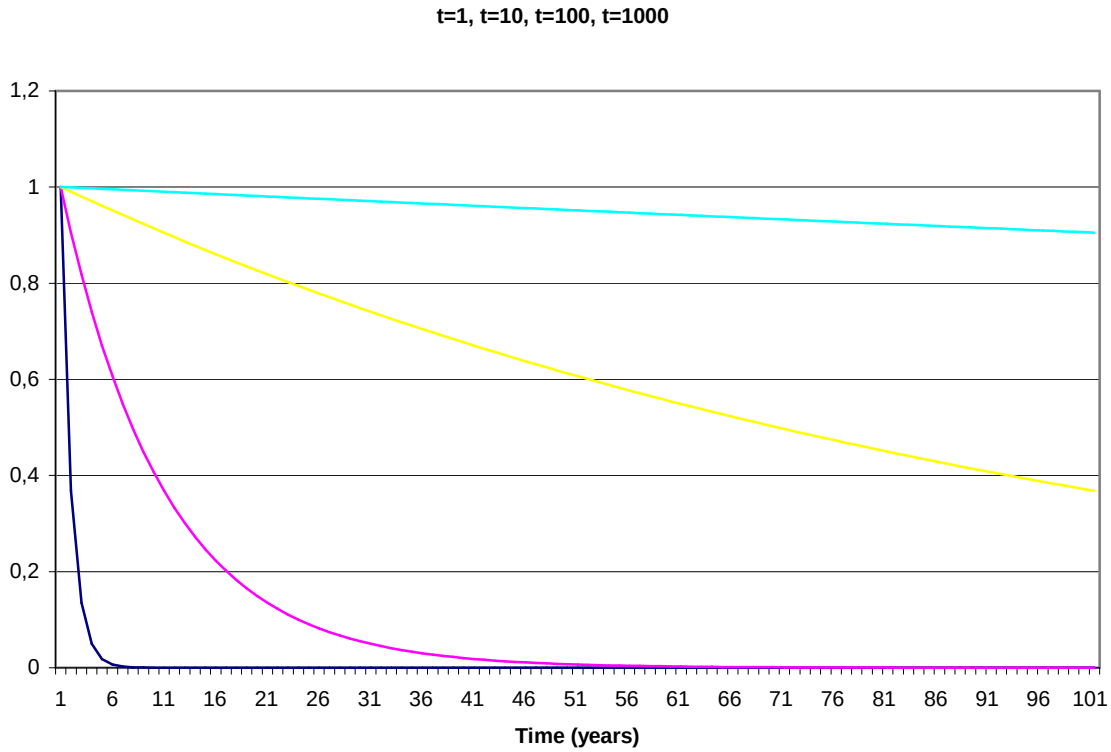
t=1, t=10, t=100, t=1000
1,2
1
0,8
0,6
0,4
0,2
0
1 6 11 16 21 26 31 36 41 46 51 56 61 66 71 76 81 86 91 96 101
Time (years)

a)

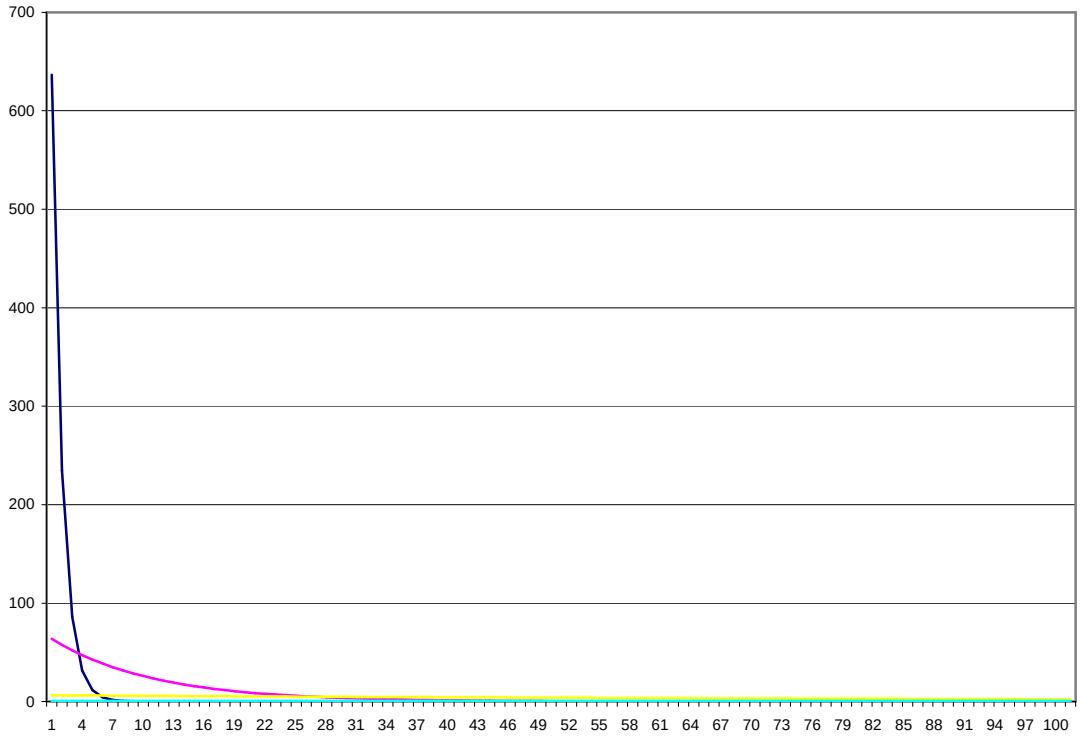
700
600
500
400
300
200
100
0
1 4 7 10 13 16 19 22 25 28 31 34 37 40 43 46 49 52 55 58 61 64 67 70 73 76 79 82 85 88 91 94 97 100

b)

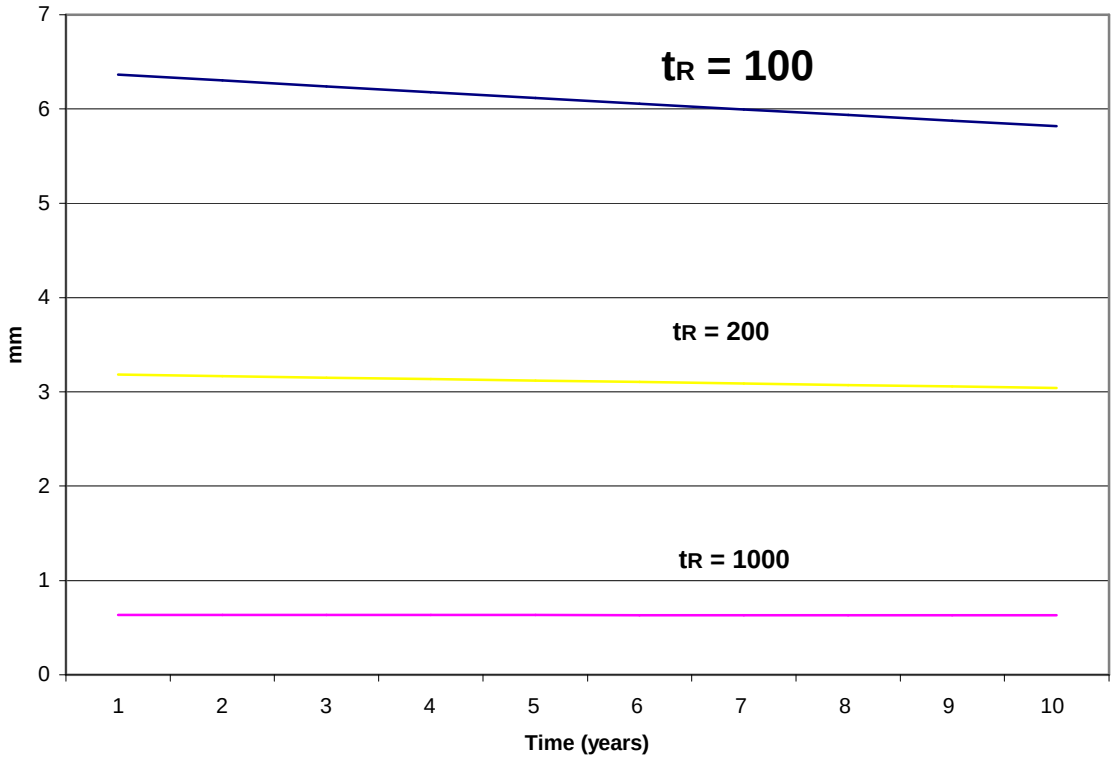

c)

Figure 12. eq. 6 a) $\exp(-t/\tau_R)$, τ_R from 1 to 1000 years;
b) $(\Delta u/\pi \cdot \tau_R) \cdot \exp(-t/\tau_R)$ in mm, τ_R from 1 to 1000 years;
c) $(\Delta u/\pi \cdot \tau_R) \cdot \exp(-t/\tau_R)$ in mm, zoom for τ_R from 100 to 1000 years.

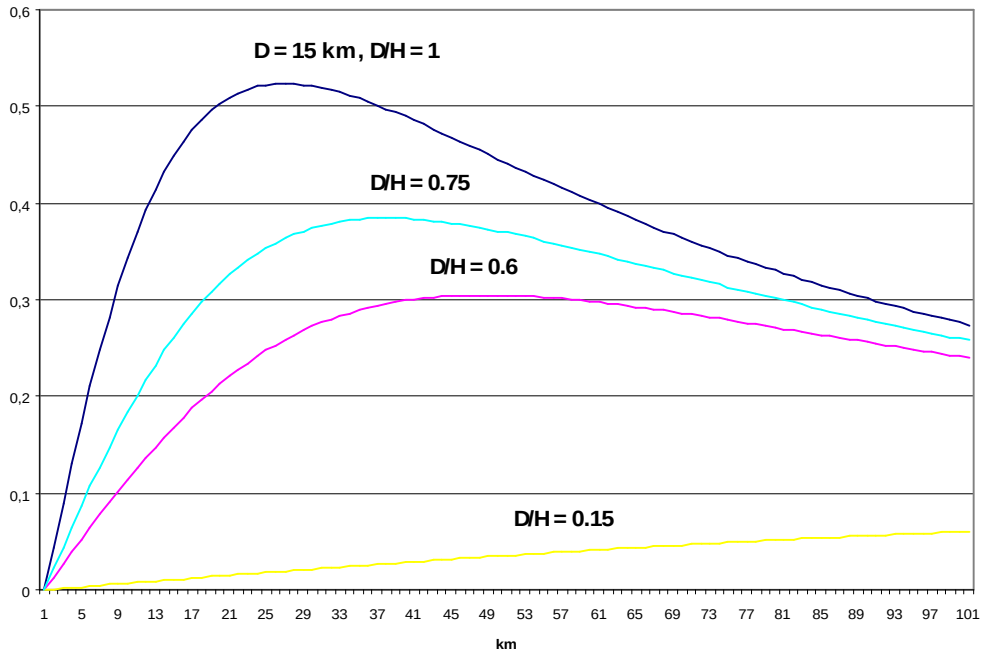

Figure 13. Spatial distribution $F_1(x, D, H) = \tan^{-1}[2xD/x^2 + (2H)^2 - D^2]$ in eq. 6 at distances x from the fault up to 100 km.

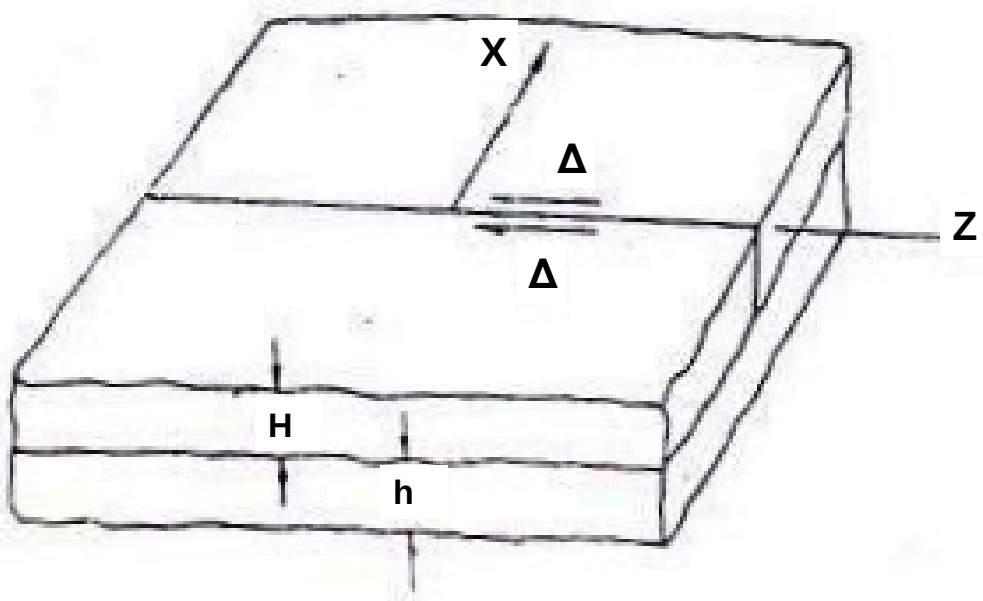

Figure 14. Two layers Elsasser model.